Digital Elevation Model with the Ground-based SAR IBIS-L as Basis for Volcanic Deformation Monitoring

Sabine Rödelsperger, Matthias Becker, Carl Gerstenecker, Gwendolyn Läufer, Kathrin Schilling, Dieter Steineck

Accepted Manuscript

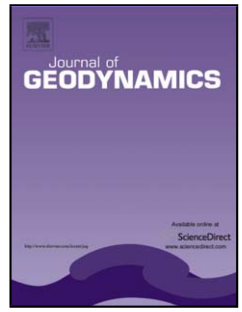

Title: Digital Elevation Model with the Ground-based SAR IBIS-L as Basis for Volcanic Deformation Monitoring

Authors: Sabine Rödelsperger, Matthias Becker, Carl Gerstenecker, Gwendolyn Läufer, Kathrin Schilling, Dieter Steineck

PII: S0264-3707(09)00142-2
DOI: doi:10.1016/j.jog.2009.10.009
Reference: GEOD 947

To appear in: *Journal of Geodynamics*

Received date: 18-12-2008
Revised date: 22-10-2009
Accepted date: 29-10-2009

Please cite this article as: Rödelsperger, S., Becker, M., Gerstenecker, C., Läufer, G., Schilling, K., Steineck, D., Digital Elevation Model with the Ground-based SAR IBIS-L as Basis for Volcanic Deformation Monitoring, *Journal of Geodynamics* (2008), doi:10.1016/j.jog.2009.10.009

Digital Elevation Model with the Ground-based SAR IBIS-L as Basis for Volcanic Deformation Monitoring

Sabine Rödelsperger*[1], Matthias Becker[1], Carl Gerstenecker[1], Gwendolyn Läufer[1], Kathrin Schilling[2], Dieter Steineck[3]

1) Institute of Physical Geodesy, Technische Universität Darmstadt, Petersenstrasse 13, 64287 Darmstadt, Germany

2) i3mainz, FH Mainz, Holzstrasse 36, 55116 Mainz, Germany

3) Institute of Photogrammetry and Cartography, Technische Universität Darmstadt, Petersenstrasse 13, 64287 Darmstadt, Germany

* Corresponding author: Tel.: +49 6151 16 6560, Fax: +49 6151 16 4512,

eMail: roedelsperger@geod.tu-darmstadt.de

Abstract

Within the project Exupéry, a hybrid deformation observation system is developed, which is part of a Volcano Fast Response System (VFRS). The VFRS shall be a mobile, robust, real-time, easy to use early warning system, which, in case of a volcanic crisis, will support the locale authorities in their decisions about hazard mitigation provisions, especially about the evacuation of people.

The hybrid deformation observation system combines a ground-based Synthetic Aperture Radar named IBIS-L with a network of GPS receivers and will allow the continuous, weather independent determination of areal 3D displacements.

In this paper we present the results of first tests with IBIS-L in an active quarry near Dieburg, Germany. A Digital Elevation Model (DEM) was determined with IBIS-L and compared with a DEM derived by terrestrial laserscanning and photogrammetry. The ability to determine accurate DEMs with IBIS-L is the basis for the combination of different observation techniques, as without a DEM the displacements observed with IBIS-L cannot be georeferenced.

The standard deviation of the differences between the DEM by IBIS-L and the DEM by laserscanning and photogrammetry depends on the surface characteristics. We found a standard deviation of 0.8 m at a slope of rocks and debris, 2.0 m at mining terraces with low vegetation and 3.0 m in a vegetation covered area.

Keywords: Ground-based Synthetic Aperture Radar (GB-SAR), IBIS-L, Digital Elevation Model (DEM), Atmospheric effect, Volcano Fast Response System

Introduction

Within the framework of the German research program "Geotechnologien", funded by the Bundesministerium für Bildung und Forschung (BMBF), the multi-disciplinary project Exupéry has the aim to develop a mobile Volcano Fast Response System (VFRS) for hazard mitigation (see http://www.geotechnologien.de and http://www.exupery-vfrs.de).

The system allows a quick deployment at any volcano in case of indications for a volcanic crisis or volcanic unrest. The core of the VFRS consists of well-known volcanic monitoring techniques, both space and ground based, to observe seismicity, ground deformation, gas emissions and thermal activity. All data are processed in near real-time and stored in a central data base. Models will be derived to determine the actual state of activity and to set alert levels. The different tasks of Exupéry are described in more detail in Zaksek et al. (2008).

Within the Exupéry project, the Institute of Physical Geodesy, Technische Universität Darmstadt, Germany develops a hybrid ground based sensor system to monitor displacements of the volcano surface. Such a system has to fulfil certain requirements as:

- high mobility to enable a quick deployment of the system
- weather independent continuous and automated monitoring
- high temporal and spatial resolution
- real-time evaluation

Classical approaches for monitoring ground deformation (e.g. extensometers, inclinometers, tiltmeters) require the installation in the volcanic area which might be inaccessible during a volcanic crisis. Therefore the system consists of a network of dual and single frequency GPS receivers in combination with a Ku-band ground-based Synthetic Aperture Radar (GB-SAR) named IBIS-L. The low-cost single-frequency GPS receivers will be stationed inside the radar beam, while the precise dual frequency receivers form the base network. In a new processing approach a joined analysis of discrete GPS data and areal interferometric SAR data, will deliver georeferenced areal deformation in real-time with a spatial resolution of several meters and a temporal resolution of several minutes.

Many studies show the potential of GB-SAR in applications like displacement monitoring at landslides (e.g. Luzi et al., 2006, Antonello et al., 2004), avalanches (e.g. Martinez-Vazquez and Fortuny-Guash, 2005) and glaciers (e.g. Noferini et al., 2009). The advantage compared to optical remote sensing instruments is the ability to monitor areal displacements at any weather condition independent on daylight with a measurement accuracy of 0.1 to 1 mm.

A further application of GB-SAR is the generation of a Digital Elevation Model (DEM) (e.g. Pieraccini et al., 2001, Noferini et al., 2007). The possibility to generate a DEM with IBIS-L is very important within the Exupéry project. The goal of the project is to combine several observation techniques to determine the actual condition of a volcano, which necessitates a common reference system. A DEM is required to georeference the measured displacements with IBIS-L, i.e. to project the displacements into the common reference system. As result of the Shuttle Radar Topography Mission (SRTM) a DEM with a ground resolution of 90 x 90 m is globally available for free.

This resolution is, however, not sufficient for our application. This paper focuses on the generation of a DEM with IBIS-L which is the basis for the combined displacement monitoring of IBIS-L and GPS.

IBIS-L

IBIS-L (Image By Interferometric Survey) is a GB-SAR device developed by IDS, Pisa, Italy. It consists of a Stepped-Frequency Continuous-Wave radar unit, operating at 17.2 GHz (Ku-band) with a bandwidth of 200 MHz. The synthetic aperture is realized by the movement of the radar unit along a linear rail of 2 m length. The result of one scan along the entire rail is a two dimensional image containing amplitude and phase with a maximum resolution of 0.75 m in range and 4.5 mrad in cross-range (i.e. 4.5 m at 1 km distance to the sensor). The maximum observation range is 4 km.

An interferogram is formed by computing the difference between the phase images of two scans at different times. The observed interferometric phase ϕ_{obs} of each pixel is a sum of several effects

$$\phi_{obs} = \phi_{topo} + \phi_{disp} + \phi_{atm} + \phi_{noise} \qquad (1)$$

where ϕ_{topo} is the phase difference due to topography, ϕ_{disp} the displacement in line-of-sight (LOS), ϕ_{atm} the atmospheric disturbance and ϕ_{noise} the instrumental noise and unmodelled effects (i.e. variations of dielectrical properties of the surface).

In contrast to spaceborne SAR, the spatial baseline (i.e. the distance between the two antenna positions in one interferogram) can be selected consciously, depending on the application.

The zero-baseline condition (i.e. spatial baseline is zero) is the ideal condition for displacement monitoring because then ϕ_{topo} is zero.

If the spatial baseline is not zero, a DEM can be derived from ϕ_{topo}. Assuming a spatial baseline only in vertical direction, the relation between elevation z and phase difference ϕ_{topo} of one particular pixel can be approximated by (Noferini et al., 2007)

$$z = \frac{\lambda \phi_{topo}}{4\pi} \frac{r}{B} \qquad (2)$$

with λ being the wavelength, r the distance to the target and B the vertical baseline.

In case of IBIS-L a spatial baseline length between 0.025 and 0.1 m is possible.

IBIS-L delivers amplitude and phase organized in a two dimensional array of pixels with range and cross-range resolution. Assuming that the position and the orientation of IBIS-L is known, a DEM of the illuminated area is necessary to transform the array of amplitude and phase into the common reference system. The error of the projected positioning σ_x in LOS onto the DEM depends on the error of elevation σ_z and the elevation angle β of the target with reference to IBIS-L (see Figure 1)

$$\sigma_x = \sigma_z \tan\beta \tag{3}$$

DEM generation

To determine a DEM with IBIS-L, the phase difference ϕ_{topo} has to be extracted from the observed interferometric phase ϕ_{obs}. As stated in formula (1), additionally to the topography, the observed interferometric phase is also subjected to LOS displacements, instrumental noise and atmospheric disturbances.

Due to the short temporal baseline (i.e. time interval between the images) of about 5 to 10 minutes, the LOS displacements are assumed to be zero. Assuming the instrumental noise to be white noise, the noise can be reduced considerably with the stacking of repeated measurements.

Even with short temporal baselines, the atmospheric effect cannot be neglected. Different methods exist to account for the atmospheric path delay (e.g. Zebker et al., 1997, Luzi et al., 2004).

Assuming constant atmospheric conditions along the path, the path delay Δr can, according to Zebker et al. (1997), be approximated by

$$\Delta r = \left(7.76 \cdot 10^{-5} \cdot \frac{P}{T} + 3.73 \cdot 10^{-1} \cdot \frac{e}{T^2}\right) \cdot r \tag{4}$$

whereas P is the atmospheric pressure in hPascal, T the temperature in Kelvin, e the partial pressure of water vapour in hPascal and r the path length.

The assumption of constant atmospheric conditions along the path results in a linear model

$$\Delta r = c(t) \cdot r \tag{5}$$

with $c(t)$ being constant for all pixels at time t and determined as stated in equation (4).

Whether the approach with a linear model is sufficient or not depends on the conditions of the site. Especially the maximum range and the look angle play an important role in the decision of the method for the estimation of atmospheric effects. With great distances and steep look angles non-linearities (e.g. spatial variations of the atmosphere) have to be taken into account. The corrected phase difference is still wrapped within the range $-\pi$ to $+\pi$. To retrieve the unwrapped phase difference ϕ_{uw} of one particular pixel, the absolute offset (i.e. an integer multiple of 2π) has to be determined

$$\phi_{uw} = 2\pi \cdot n + \phi \qquad (6)$$

with n being the unknown integer.

Here, a conventional branch cut algorithm as described in Goldstein et al. (1988) was used for the phase unwrapping. The branch cut algorithm is a path-following method, which works very well for data with high coherence. With a larger spatial baseline a better accuracy can be achieved but the phase unwrapping is more difficult since the height of ambiguity is smaller. The height of ambiguity is the height z which corresponds to one fringe, i.e. a phase change of $\phi_{topo} = 2\pi$ in equation (2) (e.g. Bamler and Hartl 1998, Noferini et al. 2008).

DEM generation at a test site

The selected test site is an active quarry in Dieburg owned by the Odenwälder Hartstein Industrie (see Figure 2 a). The coherence of this scene is shown in Figure 2 b).

For the validation of the DEM derived from IBIS-L, a reference DEM was determined by a combination of terrestrial photogrammetry and laser scanning. The laser scan was performed with a Leica HDS 3000 and the photos were taken with the Wild camera P31. The specifications of the used camera and laser scanner are listed in Table 1 and Table 2, respectively.

Both methods delivered point clouds which were registered and combined by transformation with a set of identical control points. The comparison of both DEMs yields a standard deviation of 0.07 m in areas where rock and debris dominate and a standard deviation of 0.41 m where vegetation is present. The combined DEM is shown in Figure 4 a.

With IBIS-L, 45 interferograms where acquired with vertical baselines of 0.05 and 0.1 m. The specifications are given in Table 3.

Before the generation of the DEM, the atmospheric effects were accounted for by applying equation (4). A weather station logged humidity, temperature and pressure at the IBIS-L station. Estimations showed that a linear model is sufficient in this test area with a maximum distance of 300 m and an almost horizontal look angle. At this distance the error caused by a change in humidity of 1 % at 25°C is almost 2.5 m in height. Here, during the measurement campaign with duration of 4.5 hours, the temperature rose by about 10°C while humidity dropped by about 20%. This shows the importance of considering atmospheric effects.

Figure 3 shows the observed phase of two control points before and after atmospheric correction. Control point 1 is a triangular reflector (edge length 0.22 m) at a distance of 100 m, control point 2 is quadrangular reflector (edge length 0.22 m) at a distance of 300 m (see also Figure 2). The jumps in the time series are induced by the introduction of a spatial baseline. Since control point 1 is 1 m lower than the IBIS instrument the jump is negative. Especially in the last section where the observed phase should be zero (because spatial baseline = 0 m), the amount of atmospheric disturbance is clearly visible. The lower graph shows the applied atmospheric correction, whereas the correction for control point 2 is three times higher than for control point 1 (due to the linear model).

The standard deviation of the corrected observation is 0.04 rad for control point 1 and 0.12 rad for control point 2. This leads to an error in height of 0.05 m for control point 1 and 0.11 m for control point 2 with a baseline of 0.1 m. The error doubles for a baseline of 0.05 m.

All possible interferograms were formed and averaged, which resulted in one mean interferogram for each baseline (0.05 and 0.1 m). The DEMs were computed using equation

(2). The standard deviation of the difference between the DEMs with baseline 0.05 and 0.1 m is 1.0 m. The final DEM derived from IBIS-L (average of both single DEMs) is shown in Figure 4 b. The difference between the reference DEM and the IBIS-DEM is shown Figure 5 a. The mean absolute deviation is 1.8 m. 50 % of the differences are below 0.4 m. Figure 5 b shows the histogram of differences. The corresponding standard deviation is 2.5 m.

To better understand the differences, the test site is classified into four zones A-D (see Figure 2). Table 4 shows a summary of the different zones and their accuracy. Zone A is a slope with an angle of 40°, which mainly consists of rocks, debris and low vegetation (e.g. grass). The mean coherence is 0.8 ± 0.06 and the found standard deviation 0.8 m. Applying equation (3), the positioning accuracy of georeferencing for an elevation angle of 20° is 0.3 m, which is below the spatial resolution of IBIS-L.

Zone B is an old mining area consisting of four terraces with almost vertical walls. The top of each terrace is covered with low vegetation, e.g. bushes and low trees. The mean coherence of this area is with 0.7 not bad but the variation (coherence standard deviation 0.23) is very high due to the covering with vegetation. The standard deviation of height amounts to 2.0 m which leads to positioning accuracy of 0.7 m for an elevation angle of 20°. In general, vertical walls are not represented well in a conventional DEM.

Zone C is mainly covered with vegetation as bushes and trees. The mean coherence is 0.5 ± 0.22. Large discrepancies can be found here, which is expected because vegetation is moving constantly due to wind and thus increases the noise. In this zone the standard deviation amounts to 3.0 m which corresponds to a positioning accuracy of 1.0 m for an elevation angle of 20°.

Zone D only consists of rocks and the coherence is very high but this area was dug off between the measurements of the IBIS-L DEM and reference DEM because more than one month passed by. So, differences of more than ten meters can be found between both DEMs, which are no indication for the measurement accuracy.

Conclusion and outlook

A DEM was generated out of the IBIS-L measurements after the atmospheric effects were removed. A comparison with a reference DEM derived from terrestrial laserscanning and photogrammetry resulted in standard deviations of 0.8 m to 3.0 m depending on the character of the target. The best agreement between both DEMs was found at a slope of rocks and debris. As expected, low coherence targets (e.g. vegetation) decreases the accuracy of the IBIS-DEM considerably. The accuracy of photogrammetry and laserscanning may, however, suffer similar problems in areas with vegetation.

The advantage of using a DEM generated by IBIS-L for georeferencing versus a DEM retrieved from other techniques is clearly that no further measurement instrument is necessary and that the DEM has the same pixel geometry and resolution as the displacement images (i.e. interpolation is unnecessary). The disadvantage is the lower accuracy, especially in areas with low coherence. In areas without vegetation, the positioning accuracy of georeferencing is between 0.3 and 0.7 m in a maximum range of 300 m. Since the maximum achievable resolution in range is 0.75 m with IBIS-L, the accuracy is sufficient.

Further investigations have to be made concerning the accuracy in greater distances. Noferini et al. (2007) achieved a standard deviation of 5.5 m with C-band SAR in 2 km distance, which corresponds to a positioning accuracy of 2 m. As Ku-band SAR, the measurement accuracy of IBIS-L is higher but it also suffers more from atmospheric disturbance and decorrelation.

Here we have shown for the first time the generation of a DEM with a Ku-band GB-SAR IBIS-L and compared it with a high accuracy reference DEM by terrestrial photogrammetry and laser scanning. The goal of the volcano monitoring system is to combine the areal LOS displacements of IBIS-L with 3D displacements measured by GPS. The possibility to generate a DEM is an important step towards this combined analysis, as it enables us to project the particular pixels of IBIS-L images and their displacements to a common reference system. It is the basis for the monitoring of 3D areal displacement, whereas GPS delivers the third dimension at particular points.

Acknowledgments

The authors thank the Odenwälder Hartstein Industrie for permitting us the installation of IBIS-L in the quarry in Dieburg. This project is funded by the Bundesministerium für Bildung und Forschung within the Geotechnologien program.

References

Antonello, G., Casagli, N., Farina, P., Leva, D., Nico, G., Sieber, A. and Tarchi, D. (2004): Ground-based SAR interferometry for monitoring mass movements. Landslides 1, pp. 21-28.

Bamler, R. and Hartl, P. (1998): Synthetic aperture radar interferometry. Inverse Problems 14, R1-R54.

Goldstein, R.M., Zebker, H.A. and Werner, C.L. (1988): Satellite radar interferometry: two-dimensional phase unwrapping. Radio Science 23 (4), pp. 713-720.

Luzi, G., Pieraccini, M., Mecatti, D., Noferini, L., Guidi, G., Moia, F. and Atzeni, C. (2004): Ground-based radar interferometry for landslides monitoring: Atmospheric and instrumental decorrelation sources on experimental data. IEEE Transactions on Geoscience and Remote Sensing 42, pp. 2454-2466.

Luzi, G., Pieraccini, M., Mecatti, D., Noferini, L., Macaluso, G., Galgaro, A. and Atzeni, C. (2006): Advances in ground-based microwave interferometry for landslide survey: a case study. International Journal of Remote Sensing 27, pp. 2331-2350.

Martinez-Vazquez, A. and Fortuny-Guash, J. (2005): Monitoring structural changes and Stability of the snow cover with a Ground-based Synthetic Aperture Radar, Proceedings of URSI Commission F Symposium on Microwave Remote Sensing of the Earth, Ocean, Ice and Atmosphere, 20-21 April, Ispra, Italy.

Noferini, L., Pieraccini, M., Mecatti, D., Macaluso, G., Luzi, G. and Atzeni, C. (2007): DEM by Ground-Based SAR Interferometry. Geoscience and Remote Sensing Letters 4 (4), pp. 659-663.

Noferini, L., Mecatti, D., Macaluso, G., Pieraccini, M. and Atzeni, C. (2009): Monitoring of Belvedere Glacier using a wide angle GB-SAR interferometer. Journal of Applied Geophysics 68 (2), pp. 289-293.

Pieraccini, M., Luzi, G. and Atzeni, C. (2001): Terrain mapping by ground-based interferometric radar. IEEE Transactions on Geoscience and Remote Sensing 39, pp. 2176-2181.

Zaksek, K., Hort, M. and the Exupery Team(2008): Exupery: The mobile Volcano Fast Response System. IEEE proceedings of 2nd USEReST Workshop, 11-14 November, 2008, Naples, Italy.

Zebker, H.A., Rosen, P.A. and Hensley, S. (1997): Atmospheric effects in interferometric synthetic aperture radar surface deformation and topographic maps. Journal of Geophysical Research 102 (B4), pp. 7547-7563.

Figures

Figure 1: Influence of the error of elevation on the projected position.

Figure 2: Picture (a) and coherence (b) of the observed scene covered by the antenna beam in a quarry in Dieburg. The continuous line is the area of the DEM derived from IBIS; the dashed line represents the area of the DEM derived from photogrammetry and laserscanning.

Reflector 1 and 2 indicate two control points. The different zones, named A to D are described in the text.

Figure 3: Phase of the two control points 1 (+) and 2 (x) in 100 and 300 m distance, respectively. The upper graph shows the observed phase measurements (grey) and the phase after atmospheric correction (black). In the lower graph the applied atmospheric correction for both control points is plotted.

Figure 4: DEM generated by photogrammetry and laserscanning (a) and by IBIS-L (b).

Figure 5: Comparison of DEM derived from IBIS-L and the combination of photogrammetry and laserscanning in m (a). The histogram shows the distribution of differences (b).

Tables

Table 1: Specifications of the camera at the test site in Dieburg.

Camera	Wild P31
Focal length	20 cm
Scanned pixel size	15 µm
Number of reference points	4
Baseline	30 m
Maximum distance	200 m
Accuracy of height measurement	3 cm

Table 2: Specifications of the laserscanner at the test site in Dieburg.

Laserscanner	Leica HDS 3000
Instrument type	Pulsed
Maximum distance	300 m
Maximum field-of-view	360° x 270°
Accuracy of single measurement - Position - Distance	 6 mm at 50 m 4 mm at 50 m
Used resolution	3 cm at 50 m
Used max. distance	110 m

Table 3: Specifications of IBIS-L at the test site in Dieburg.

Maximum distance	300 m
Scan length	2 m

Center frequency	17.2 GHz
Bandwidth	200 MHz
Resolution	0.75 m x 4 mrad
Acquisition time	6 min
Vertical baseline	0.05 and 0.1 m

Table 4: Found accuracy of the different zones.

Zone	**Description**	**Coherence**	**Standard deviation of height**
A	Slope with rocks, debris covered with grass	0.8 ± 0.06	0.8 m
B	Mining terraces partly covered with bushes and low trees	0.7 ± 0.24	2.0 m
C	Covered with bushes and trees	0.5 ± 0.22	3.0 m
D	Working area (digging between generation of IBIS-DEM and reference DEM)	0.9 ± 0.04	-

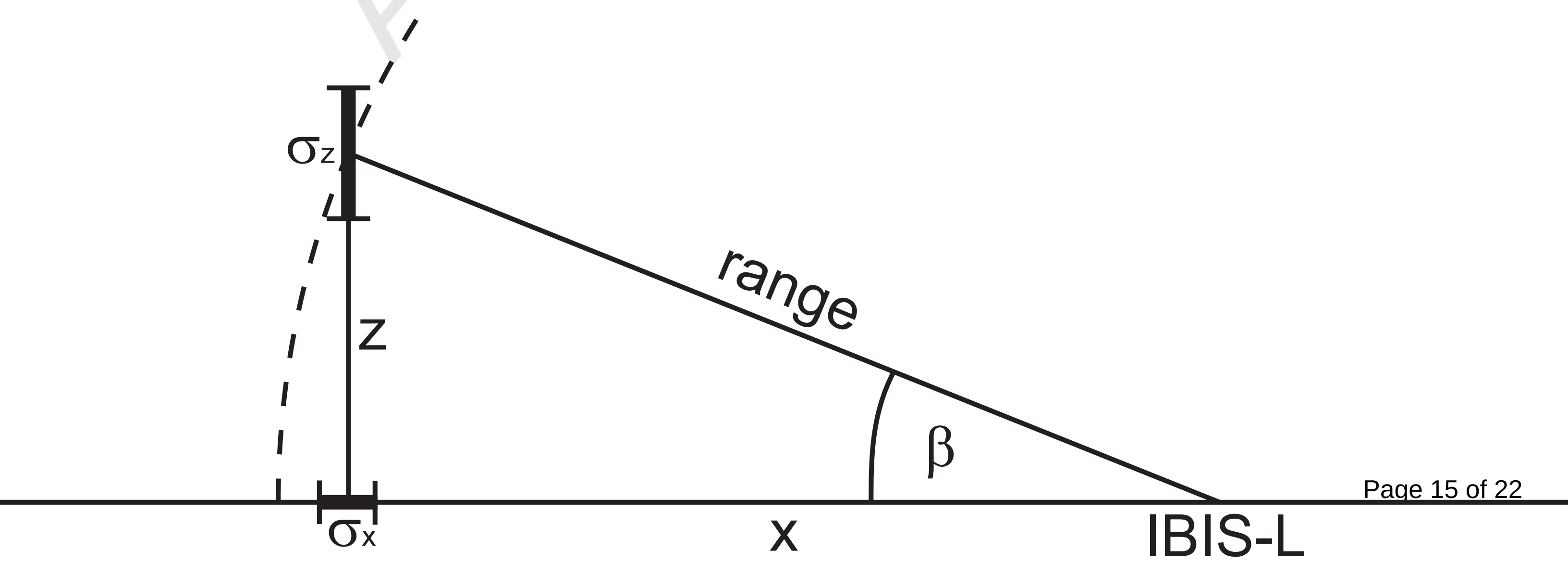
σz
z
range
β
σx
x
IBIS-L

Figure 2a

Figure 2b

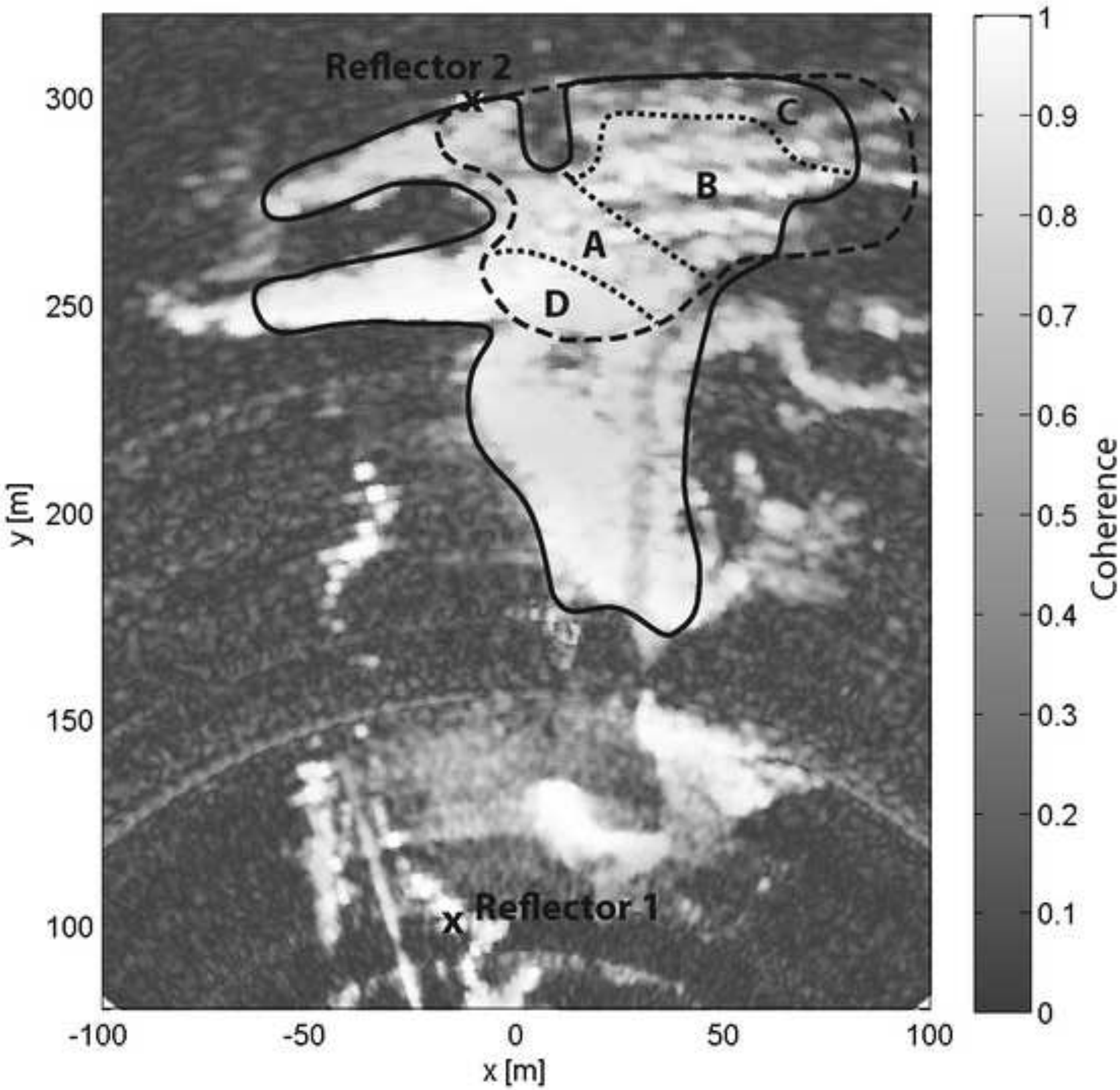

Reflector 2
Reflector 1
A
B
C
D
300
250
200
150
100
y [m]
-100
-50
0
50
100
x [m]
1
0.9
0.8
0.7
0.6
0.5
0.4
0.3
0.2
0.1
0
Coherence

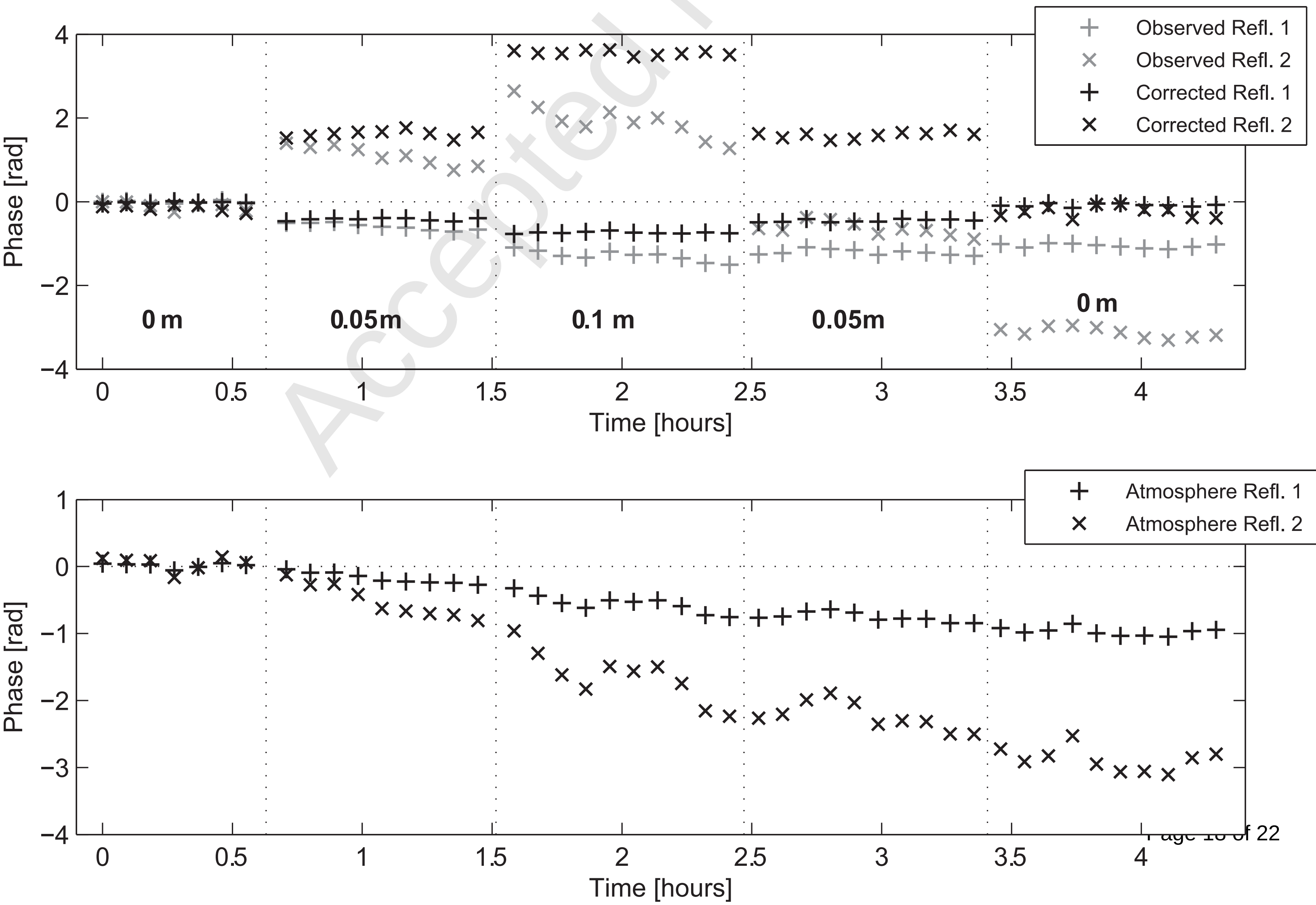
Observed Refl. 1
Observed Refl. 2
Corrected Refl. 1
Corrected Refl. 2
Phase [rad]
Time [hours]
0 m
0.05m
0.1 m
0.05m
0 m
Atmosphere Refl. 1
Atmosphere Refl. 2
Phase [rad]
Time [hours]

Figure 4a

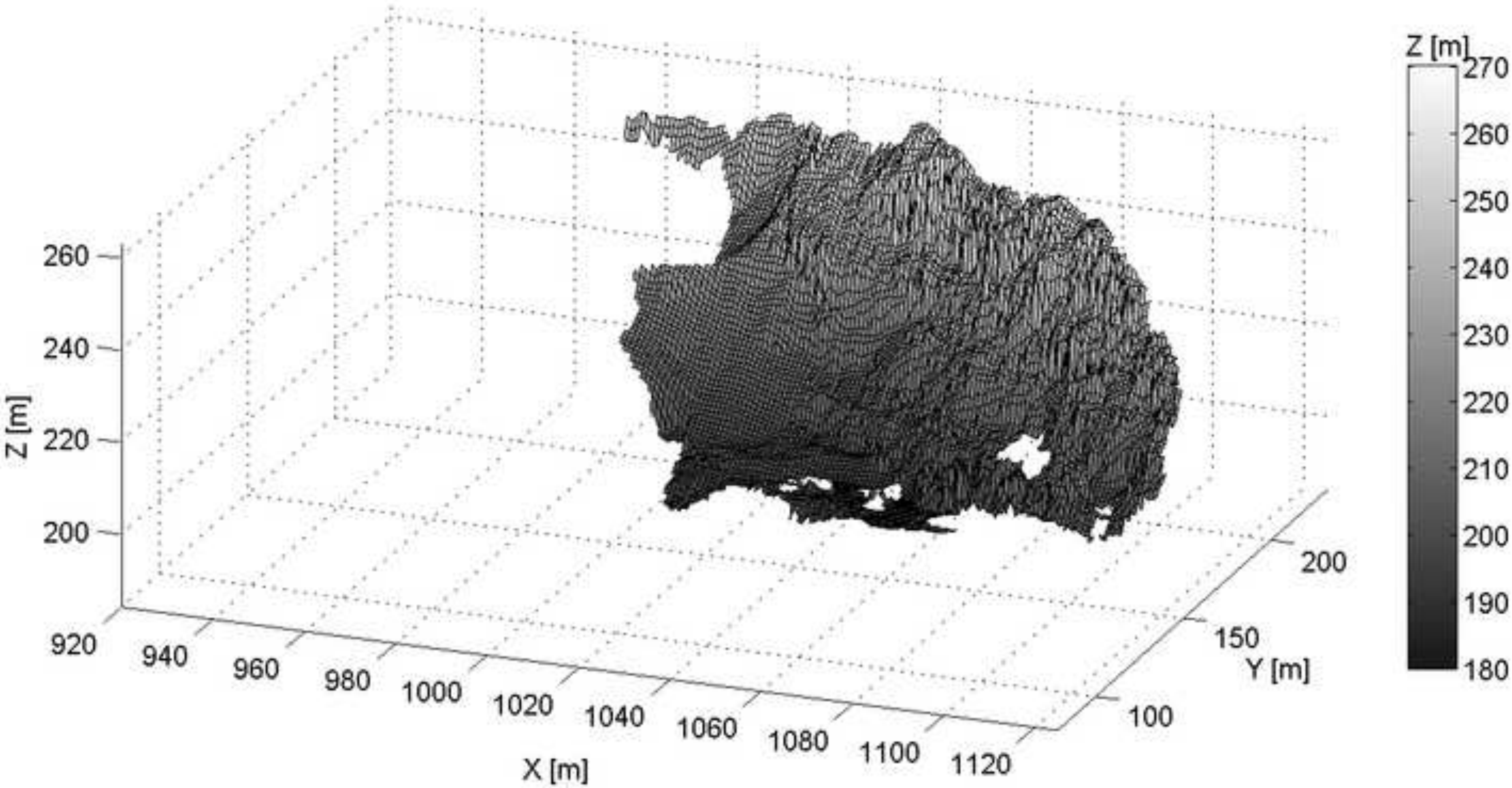
Z [m]
270
260
250
240
230
220
210
200
190
180
260
240
220
200
Z [m]
920
940
960
980
1000
1020
1040
1060
1080
1100
1120
X [m]
100
150
200
Y [m]

Figure 4b

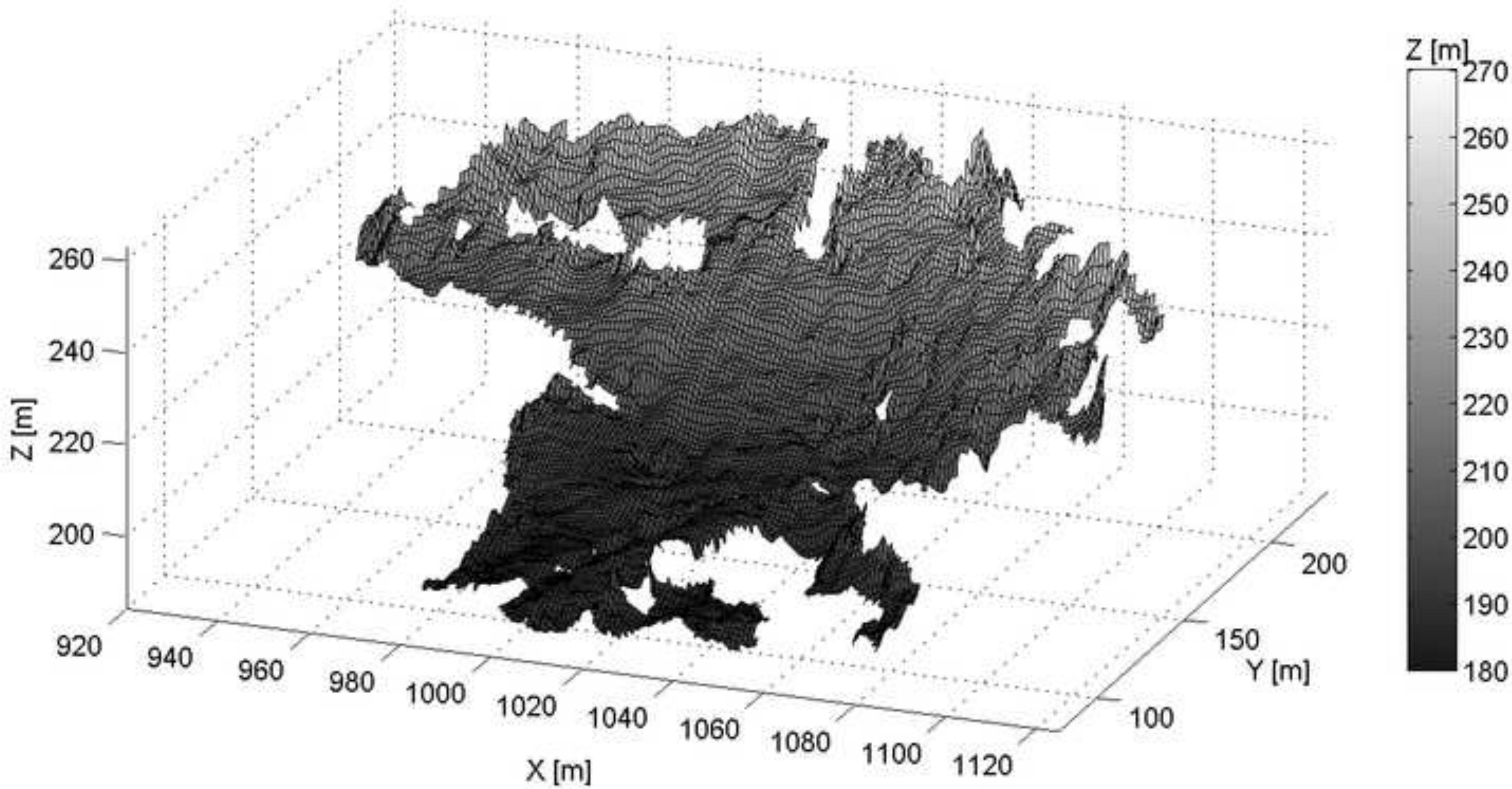

Z [m]
260
240
220
200
920
940
960
980
1000
1020
1040
1060
1080
1100
1120
X [m]
100
150
200
Y [m]
Z [m]
270
260
250
240
230
220
210
200
190
180

Figure 5a

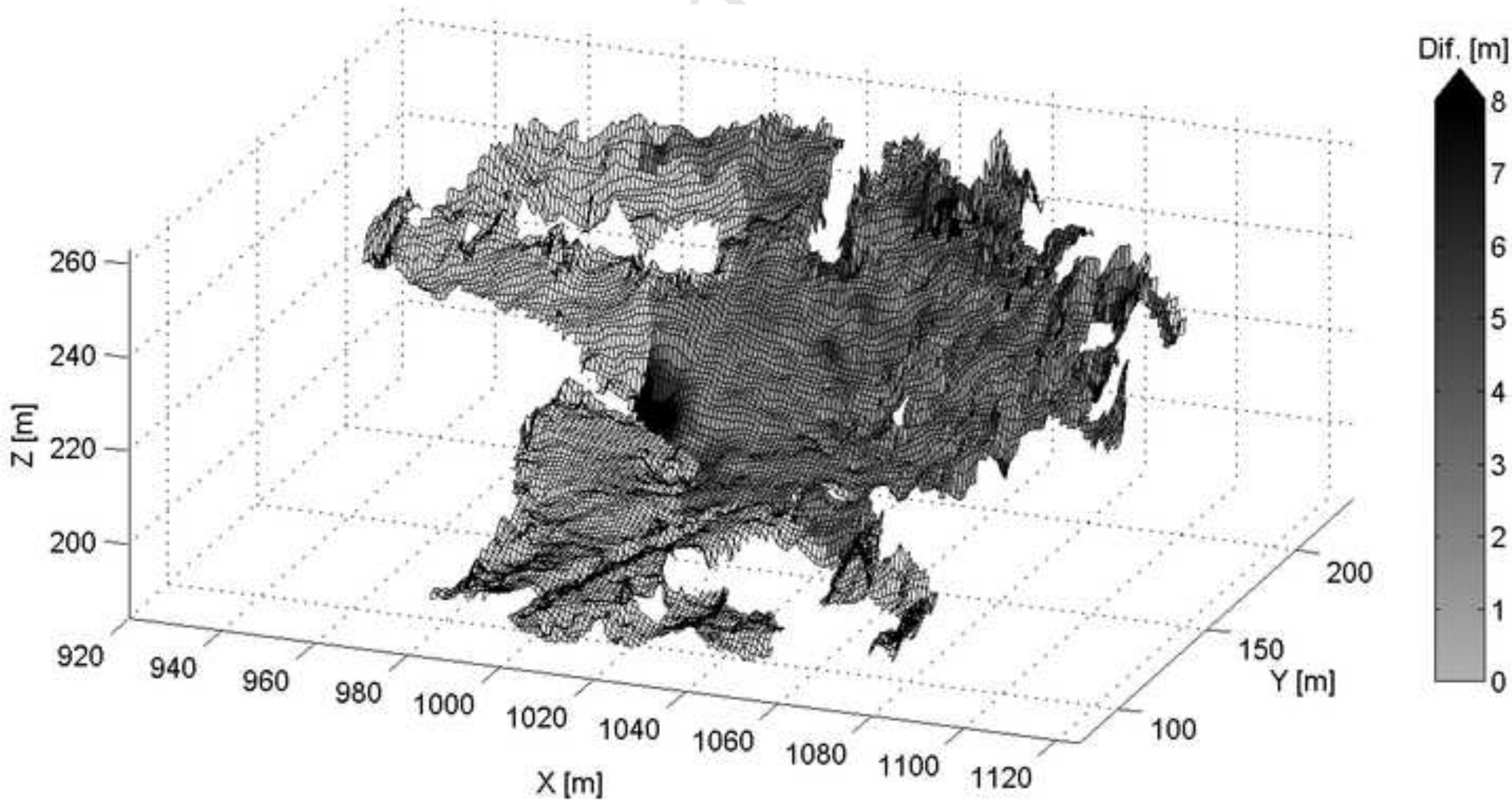

Dif. [m]
8
7
6
5
4
3
2
1
0
260
240
220
200
Z [m]
920
940
960
980
1000
1020
1040
1060
1080
1100
1120
X [m]
100
150
200
Y [m]

Figure 5b

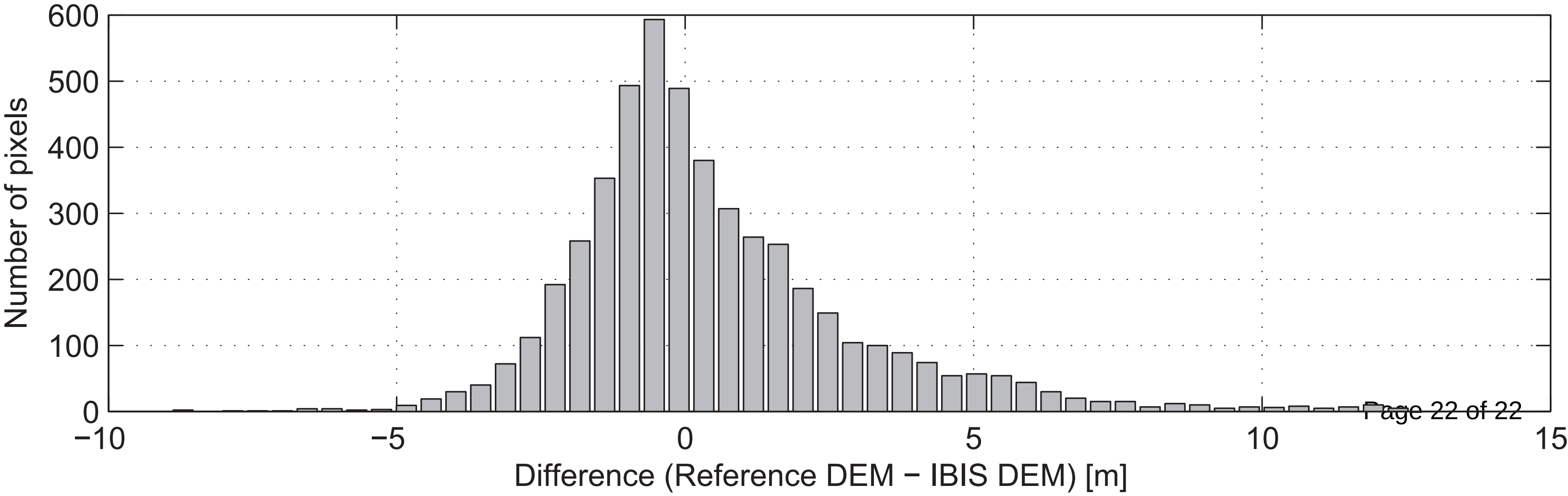
600
500
400
300
200
100
0
Number of pixels
−10
−5
0
5
10
15
Difference (Reference DEM − IBIS DEM) [m]